



## **Non-Thermal Plasmas for NO<sub>x</sub> Treatment**

Yoann-Nicolas Jaffré, Thomas Aka-Ngnui, Abderrahmane Beroual

### **► To cite this version:**

Yoann-Nicolas Jaffré, Thomas Aka-Ngnui, Abderrahmane Beroual. Non-Thermal Plasmas for NO<sub>x</sub> Treatment. IMETI, Sep 2009, Orlando, FL, United States. pp.sur CD. <hal-00410200>

**HAL Id: hal-00410200**

**<https://hal.science/hal-00410200v1>**

Submitted on 18 Aug 2009

**HAL** is a multi-disciplinary open access archive for the deposit and dissemination of scientific research documents, whether they are published or not. The documents may come from teaching and research institutions in France or abroad, or from public or private research centers.

L'archive ouverte pluridisciplinaire **HAL**, est destinée au dépôt et à la diffusion de documents scientifiques de niveau recherche, publiés ou non, émanant des établissements d'enseignement et de recherche français ou étrangers, des laboratoires publics ou privés.



HAL Authorization

# Non-Thermal Plasmas for NO<sub>x</sub> Treatment

Y.N. Jaffré, T. Aka-Ngnui and A. Beroual

Ecole Centrale de Lyon  
AMPERE C.N.R.S. UMR. 5005  
69134 Ecully Cedex, France

## ABSTRACT

This work is devoted to the determination of corona ignition threshold for non-thermal plasma generation and to the optimization of various kinds of plasma reactor geometries for exhaust gas treatment applications. The tested plasma reactor geometries were cylindrical. Some reactors have dielectric barrier made of glass or quartz in order to observe the discharges. First, the distributions of electric field and energy in reactors have been simulated. Then, current and voltage waveforms have been measured to check the discharge appearance. Geometrical singularities have been detected by both luminescence and current measurements to avoid unwanted current distortions. The experimental analysis shows the evolution of resistive and reactive components of current associated to corona discharges when increasing the voltage.

**Keywords:** Corona Discharges, Energy, Non-Thermal Plasmas, Gas Treatments

## 1 INTRODUCTION

Nitrogen oxides (NO<sub>x</sub>) are among the most important and critical pollutants that need to be reduced in exhaust gases. The present Selective Catalytic Reduction (SCR) processes can be improved for NO<sub>x</sub> reduction by a Non-Thermal Plasma (NTP) treatment. Plasmas are ionized gases, whose active species are generated by applying high electric fields in a plasma reactor. NTP alone does not reduce NO generated by a thermal engine to N<sub>2</sub> and O<sub>2</sub>, but provides an oxidation of NO to NO<sub>2</sub> upstream of a traditional Selective Catalytic Reduction. The efficiency of this system depends on two main parameters: power supply and geometry. Plasmas have been studied for gas treatment since 1980. First applications were dedicated to power plants, for example in Riace, Italy, for ENEL's coal fired electrical generation plant (Civitanò et al., 1986). Research for automotive transportation exhaust gas treatment started in the middle of the 1990's. Nowadays, the purpose is to assist the newest catalyst processes with non-thermal plasmas (NTP) to optimize the energetic consumptions and to improve the technology by mastering the discharge. This kind of treatment is of great importance since transportation exhaust gas regulations are becoming ever more stringent. European norm (standard specification) EURO 6 im-

poses a reduction of 50% on automotive NO<sub>x</sub> emissions within 2015. This paper aims at the generation and optimization of plasmas for pollution control on automotive thermal engines. In the first part, we recall some fundamental features of discharge mechanisms. The second part lights on the influence of the electric field for NTP generation and link it to the electron energies. The third part shows results of external electric field simulations. And the last part presents respectively the experimental set-up and the measurements on NTP reactor.

## 2 DISCHARGE MECHANISMS

The current versus voltage characteristic is plotted on figure 1 for DC voltage supply with an interelectrode gap of 1 cm, plane to plane electrode geometry and standard air as dielectric. Three main regions can be observed and each region corresponds to a given mode. The first mode (dark zone) is characterized by the absence of luminous phenomena and by very weak currents. The applied voltage and thence the electric field induce elastic collisions and possible ionizations due to natural or artificial radiations. Since the discharge cannot be maintained by itself, it is called "non-autonomous". The second mode is characterized by a glow, a luminous activity defined on Figure 1 as the corona discharges. The latter starts when  $U$  exceeds  $U_0$ ; thence the electric field brings sufficient energies to the electrons that ionize or dissociate molecules. Each electron newly generated contributes to electronic avalanches generation. Since the discharge propagates, the current increases, and the voltage falls down. Arc discharges involve high currents. The electrical energy consumption is the highest where arc discharges occur. The arc regime can be linked up with short circuits. Note that for the above conditions, the dielectric strength is of about 30kV/cm. Dark and Arc discharges have no interest for NTP generation. Dark discharges do not lead to oxidation or reduction processes. Arc discharges induce thermal mechanisms, high electrical energy consumptions and device destructions.

## 3 NTP PHENOMENA KNOWLEDGE

Our purpose is pollution control using corona discharges. These discharges are generated when the applied voltage (hence the electric field) exceeds a threshold value higher than the ionization and dissociation voltages of the considered gas. The electrons and ions

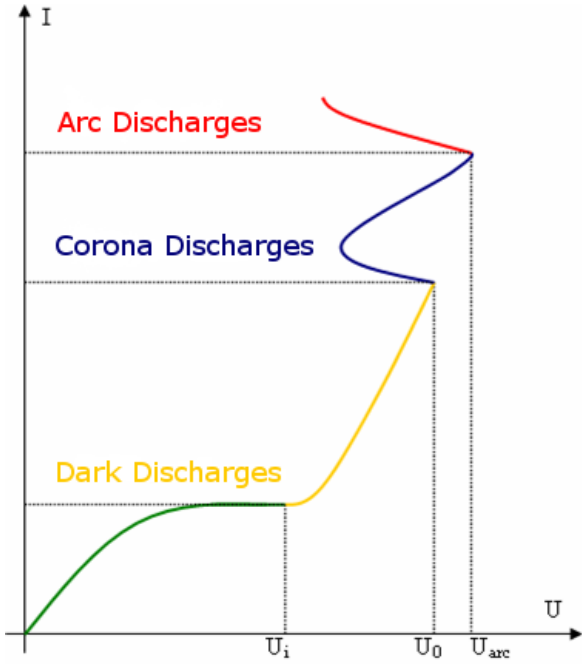


Figure 1: I-U characteristic for a uniform DC discharge

resulting from ionization drift to opposite directions. The electrons move toward the anode and the ions (positive carriers) toward the cathode. By considering the NTP conditions, neutral molecules and ions are motionless compared to the electrons. The electron mobility can be approximated from the Chapman-Enskog theory of diffusion and simplified to:

$$\mu = \frac{q}{mv} \quad (1)$$

where  $\mu$  is the mobility,  $q$  the elementary charge (electron charge),  $m$  the mass of the electron and  $v$  is the momentum transfer collision frequency. The mass of an electron is at least 2000 times less than any molecule. For an NTP, the external electric field mainly contributes to enhance electron energies. The electron drift velocities depend upon the magnitude, frequency and direction of the electric field:

$$v = \mu \cdot E \quad (2)$$

$v$  is the drift velocity and  $E$  is the external electric field. The electrons are submitted to the Lorentz force which is:

$$\vec{F} = q \cdot \vec{E} \quad (3)$$

As concerns the current density  $j$ , it is given by the following relationship:

$$j = n_e \cdot q \cdot \mu \cdot E \quad (4)$$

where  $n_e$  is the electron density. The kinetic energy of electrons is reliable to the enthalpy such as:

$$\frac{1}{2} \cdot m \cdot v = \frac{3}{2} \cdot k \cdot T_e \quad (5)$$

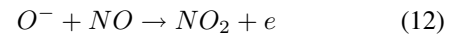
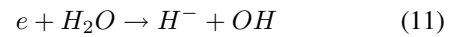
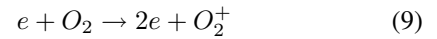
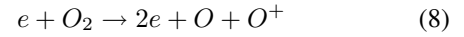
$k$  is the Boltzmann constant and  $T_e$  is the electron temperature expressed in eV ( $1\text{eV} = 1.60 \cdot 10^{-19} \text{J} = 11605 \text{K}$ ).

The statistical distribution of velocities of species is given by the Maxwell-Boltzmann statistical distribution equation. The electron energy distribution function can be defined as Maxwellian. Only a part of electrons can compete for dissociation and ionization processes. The equations above link the electron energy with the applied external electric field. By considering air at standard conditions of temperature and pressure, the physical mechanisms can be described by a series of complex equations (space charges, species interactions, transport, diffusion...). However, the external electric field remains a major parameter for NTP processes. Collisions occur according to parameters such as the energies, density of the species or collision cross sections. The mean free path of an electron is the drift distance between 2 electronic collisions:

$$\lambda = \frac{1}{n_g \cdot \sigma} \quad (6)$$

$$\lambda = \frac{v}{\nu} \quad (7)$$

$\lambda$  is the mean free path,  $n_g$  is the molecular density of the surrounding gas and  $\sigma$  is the cross section. For standard conditions in air,  $\lambda \approx 1.10^{-6} \text{m}$ ; this can lead to either slowing electrons (elastic collisions) or generating electronic avalanche (inelastic collisions). The latter suggests that a satisfying electric field can produce adequate energetic electrons. More specifically, inelastic collisions lead to internal modifications of involved species. Some examples among numerous possible reactions are listed below:



When considering a pure NO gas, the dissociation into N and O through inelastic collisions easily arises. The dissociation energy of NO is fixed at 6.5eV ([Pen93]); this value is obtained for a rough estimate electric field  $E = 5.8 \text{MV} \cdot \text{m}^{-1}$  with  $\lambda = 1.4 \cdot 10^{-6} \text{m}$ . The exhaust gases are mainly composed of  $N_2$  and  $O_2$ . Therefore, NTP does not generate a reduction but an oxidation. The oxidation takes place for energy levels above 5eV. The corona discharge ignition in the air can be calculated for cylindrical geometries from Peek formula

$$E_c = 31.8 \left( 1 + \frac{0.308}{\sqrt{\delta \cdot r}} \right) \quad (13)$$

with

$$\delta = \frac{3,92 \cdot p}{T_g} \quad (14)$$

$E_c$  is the peak value of the corona field in ( $\text{kV} \cdot \text{cm}^{-1}$ ),  $r$  is the radius of the conductor in (cm),  $p$  is the pressure in (cm.Hg) and  $T_g$  is the temperature in (Kelvin). The electric field distribution depends upon the applied voltage and the geometrical parameters. As the considered

geometry is coaxial, the electric field  $E$  can be calculated using Poisson's equation

$$\Delta V = -\frac{q}{\epsilon_0} (n_i - n_e - n_n) \quad (15)$$

$$\vec{E} = -\nabla V \quad (16)$$

$$E(r, t) = \frac{U(t)}{r \cdot \ln\left(\frac{R_{out}}{R_{in}}\right)} \quad (17)$$

Where  $V$  is the voltage potential,  $n_i$  and  $n_n$  are ion and neutral densities,  $U$  is the differential applied potential,  $r$  is the distance parameter from internal electrode,  $R_{out}$  is the external radius and  $R_{in}$  is the internal radius. Both radicals  $O$  and  $OH$  are involved in oxidation processes of  $NO$  to  $NO_2$ . These radicals are mainly produced by corona discharges in high electric field regions inducing energetic electrons according to the Maxwellian distribution of energy. But the oxidation itself takes place in low field regions during relaxing times of voltage applications or downstream of interelectrode gaps. In addition, some oxidations can appear upstream of interelectrode gaps resulting from discharge shockwaves.

## 4 CORONA DISCHARGE SIMULATIONS

Discharge depends on electrode geometries, magnitude and frequency of the voltage, electrical space charges, materials and gas parameters.

### 4.1 Geometry

In order to initiate the most efficient corona discharges for NTP generation, the geometry is highly divergent. According to equation 16 it allows high electric field while voltage magnitudes remain below 25kV. The figure 3 shows a simulation of the internal radius influence on the electric field distribution for  $U=16kV$  and external radius of 15mm. Corona discharge ignition is calculated from equation 13. The curves show that a small radius enables to get a maximum value for  $E$  substantially higher than the corona ignition, but decreasing when increasing the gap from inner electrode. For a 15mm external radius, the internal radius is ranged between 0.2 and 4.2mm. While inner radius was set as variable on Figure 3, voltage  $U$  has been set as variable on Figure 3 where  $E$  was plotted for  $R_{in}=0.35mm$  and  $R_{out}=15mm$ . The corona ignition threshold is calculated for these geometric parameters:  $E_{corona}=8.2kV/mm$ .

### 4.2 Power supply and arc limitation

The voltage has to be sustained below the disruptive voltage ( $U_d$ ). However, the arc will not occur if the voltage application time over  $U_d$  is too narrow. Streamers propagate with a non infinite velocity which means that the critical electric field can be reached by a pulse voltage during few nanoseconds but no arc. Care must be given on pulse repetition frequency, relaxing, rising and falling times. When relaxing time is too short and repetition frequency is too high, space charges can not be completely

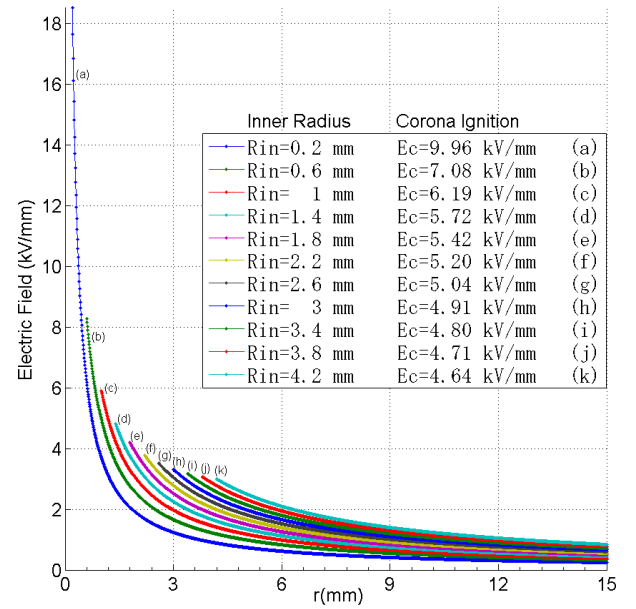


Figure 2:  $E$  vs. inner radius for  $U=16kV$  and corona ignition value

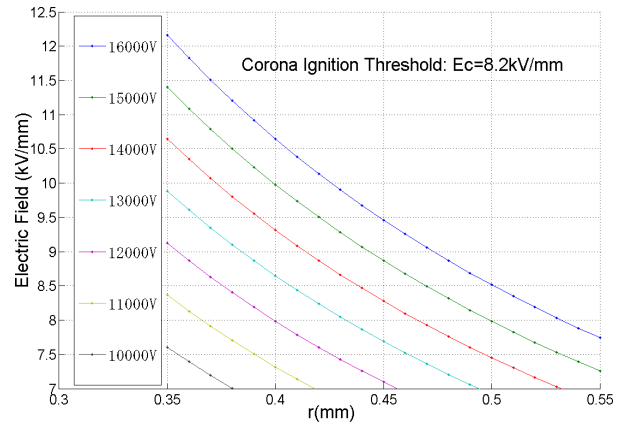


Figure 3:  $E$  vs. inner radius depending on the applied voltage

eliminated and thus arc will propagate. Short rising and falling times help for a better control of discharge. When  $E$  is suddenly applied, electrons are strongly accelerated whereas ions have a lag time. Discharge shutdown and electrical power consumption depend on falling time. This kind of power supply is hardly realizable with classic solid-state devices for voltage over 10kV but silicon carbide opens new possibilities within close future.

### 4.3 Dielectric barrier

Another method to limit arc discharges consists of adding a dielectric barrier on one or both electrodes. Glass, quartz or any translucent materials are convenient for discharge observations as shown on figure 4. DC power supply cannot be used with Dielectric Barrier Discharges (DBD) because charges settle on barrier surfaces and cancel the electric field.

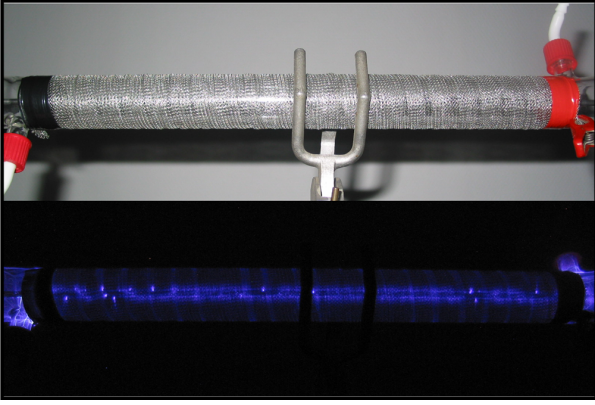


Figure 4: Corona Discharges with Glass Dielectric (DBD)

#### 4.4 Materials and gas parameters

The NTP for NO<sub>x</sub> treatment has an oxidative leading function. Materials used for the electrodes have to remain unaffected by oxidation. Tungsten or stainless steel is preferred for building reactors. Exhaust gases can have rather high temperatures according to experimentations, with a maximum temperature of 550K. The insulating materials have to be matched to these temperature and corrosive requirements. The exhaust gas is simulated using an air compressor or generated using a 4-strokes/1-cylinder fuel engine. Engine gas flow is ranged between 10l.min<sup>-1</sup> and 150l.min<sup>-1</sup>.

### 5 EXPERIMENTAL SETUP

The investigated system consists of a voltage source, a test reactor and an electrical measurement system. The voltage is measured thanks to a voltage divider, Tektronik 6015A (dividing ratio of 1000), with a bandwidth of 20MHz. The current is measured using 4 devices: 2 inductives, 1 resistive and 1 digital multimeter. The inductive devices are a transducer, Stangenes 0.5-0.1W, transforming current into voltage (ratio of 0.1V/A) with a bandwidth of 20MHz on one hand, a Rogowski coil associated to an integrator (ratio of 0.1V/A) with a bandwidth range from 100kHz to 1GHz on the other hand. The resistive sensor is configured to obtain accurate measurement of the current on a 50Ω impedance. DMM device (Digital MultiMeter) is a NI PXI-4071 measuring current with ranges from 1pA up to 3A. This is mainly used to obtain the DC component and thus complete information on complex currents generated by discharges. In order to limit the current, a protective resistance is added to the circuit as shown on figure 5. Two types of voltage sources are used: (1) DC high voltage 60kV max; and (2) AC high voltage 25kV (rms).

### 6 CORONA THRESHOLD MEASUREMENT

The measurements of high voltage currents are very sensitive. There are actual risks of arc discharges and thus the destruction of measurement devices. To avoid these

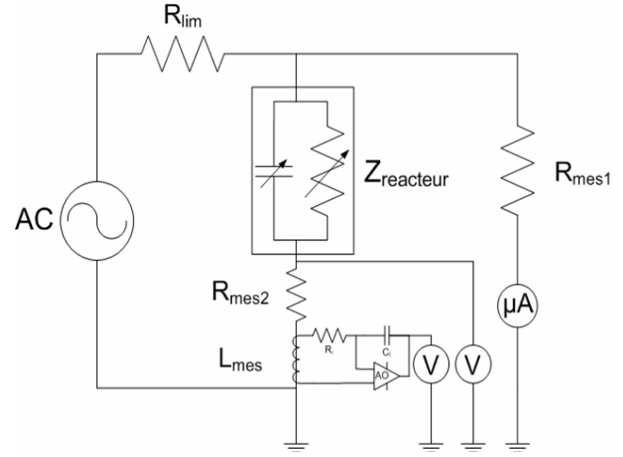


Figure 5: Equivalent Circuit of the Experimental Setup

risks, NTP reactors are subjected to a first phase of tests, where arc voltage is measured. Then, current measurements can be completed. The high frequencies of pulses formed by the discharge (whatever DC or AC) constitute another sensitive parameter. The measurements with the Stangenes transducer on a DBD reactor showed that a 20MHz bandwidth could not completely satisfy the measurements of discharge current. The threshold voltage of corona ignition is solved from equation (eq:13) and gives  $E_c = 8.2 \text{ kV/mm}$  for  $r = 0.35 \text{ mm}$ . Voltages are taken from figure 4. The latter show that in the vicinity of the inner electrode,  $E$  is over  $E_c$  for  $U = 11 \text{ kV}$  and above. The experimental results are presented on figure 6(a), 6(b), 6(c) and 6(d). The figure 6(a) is characterized by a pure capacitive current. The voltage wave is  $-90^\circ$  out of phase with the current wave and the positive current alternation is measured greater than the negative. Figure 6(b) shows the current and voltage waveforms for initially calculated corona ignition threshold. A current peak appears almost in phase with the voltage. The discharge current gets a resistive component and the current amplitude becomes substantially smaller for capacitive than for resistive components. Numerous short pulses of current appear mainly during negative alternations. Figures 6(c) and 6(d) illustrate the phenomena that increases with the applied voltage. Figure 6(c) presents a middle state between reactive and resistive periods. Figure 6(d) shows almost a sin wave of current in phase with the voltage. Note that during experimentations we used a high speed CCD camera to observe discharges and eventual singularities (hot spot) that promote current peaks and arcs. The corona ignition threshold observation is in agreement with the previous calculation with an acceptable error of 5%. Luminance generated by the corona discharges appears for  $U = 10.5 \text{ kV}$  (see figure 1). This would mean that singularities were avoided.

### 7 PROSPECTS AND CONCLUSIONS

The selective catalytic reduction (SCR) leads to NO<sub>x</sub> reduction. The products used for assisting the reactions are based on urea or hydrocarbons. The requirements to assist the reduction are the temperature and an oxidation



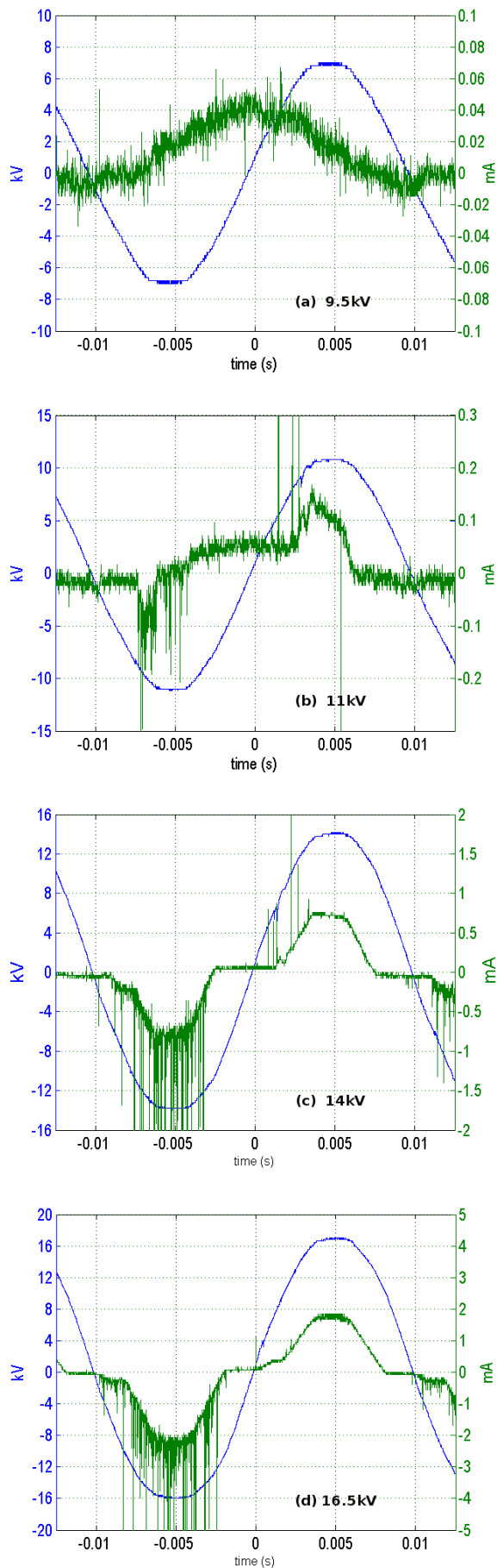


Figure 6: Current and Voltage Characteristics of AC Corona Discharges for a Wire/Cylinder Geometry, No Dielectric Barrier. Umax ranges : (a) 9.5kV, (b) 11kV, (c) 14kV, (d) 16.5kV

stage converting a part of NO to NO<sub>2</sub>. The fastest reactions with NH<sub>3</sub> can take place for NO and NO<sub>2</sub> on stoichiometric ratios of 1:1. NH<sub>3</sub> is obtained by the urea hydrolysis. But, below 200°C and during transient phases, the oxidative level doesn't work efficiently. The purpose is to create positive conditions for NOx reduction by SCR through the association with non-thermal plasmas whatever engine phases. This work contributes to discharge analysis for NTP generation. Corona discharges are well fitted for NTP reactors, but not for any voltage or geometry. In mastering electrical engineering, the combination of non-thermal plasmas and SCR has many additional advantages and promises to be a valuable economic way to treat pollutants in near future. Our researches lead to plasma technology experimentations with real exhaust gases using a thermal engine mounted on a test bench since we assumed that transient phases are not well transcribed by simulated gases.

## References

- [1] N.S.J. Braithwaite. Introduction to gas discharges. *Plasma Sources Sci. Technol*, 9(4):517–527, 2000. 2107.
- [2] J.L. Delcroix and A. Bers. *Physique des plasmas*. InterEditions, 1994.
- [3] D. Dubois, N. Merbahi, O. Eichwald, M. Yousfi, and M. Benhenni. Electrical analysis of positive corona discharge in air and n<sub>2</sub>, o<sub>2</sub>, and co<sub>2</sub> mixtures. *Journal of Applied Physics*, 101(5):053304–053304, 2007.
- [4] I. Fofana and A. Beroual. A new proposal for calculation of the leader velocity based on energy considerations. *Journal of Physics-London-D Applied Physics*, 29:691–696, 1996.
- [5] Ariège Réseau Plasmas froids France Journées d'échanges 01 Bonascre. *Plasmas froids génération, caractérisation et technologies Intégrations (Saint-Étienne)*. Publications de l'Université de Saint-Étienne, 2004.
- [6] R. Hackam and H. Aklyama. Air pollution control by electrical discharges. *IEEE Transactions on Dielectrics and Electrical Insulation*, 7(5):654–683, 2000.
- [7] W. Hartmann, M. Romheld, and K.D. Rohde. All-Solid-State Power Modulator for Pulsed Corona Plasma Reactors. *IEEE Transactions on Dielectrics and Electrical Insulation*, 14(4):858–862, 2007.
- [8] R. Ono and T. Oda. Formation and structure of primary and secondary streamers in positive pulsed corona discharge effect of oxygen concentration and applied voltage. *Journal of Physics D, Applied Physics*, 36(16):1952–1958, 2003.
- [9] F.W. Peek. *Dielectric phenomena in high voltage engineering*. McGraw-Hill Book Company, inc., 1920.

- [10] BM Penetrante, MC Hsiao, BT Merritt, GE Vogtlin, PH Wallman, A. Kuthi, CP Burkhart, and JR Bayless. Electron-impact dissociation of molecular nitrogen in atmospheric-pressure nonthermal plasma reactors. *Applied Physics Letters*, 67:3096, 1995.
- [11] B.M. Penetrante, S.E. Schultheis, North Atlantic Treaty Organization, and Scientific Affairs Division. *Non-thermal plasma techniques for pollution control*. Springer-Verlag, 1993.
- [12] T. Reess. *Contribution à l'étude expérimentale et théorique des décharges électriques de polarité négative dans l'air à la pression atmosphérique*. PhD thesis.
- [13] EM van Veldhuizen, TMP Briels, LR Grabowski, AJM Pemen, and U. Ebert. Influences of the pulsed power supply on corona streamer appearance. *2nd Int. Workshop on Cold Atmospheric Plasmas: Sources and Applications, Bruges, Belgium*, 2005. 2007.
- [14] GE Vogtlin and BM Penetrante. Pulsed corona discharge for removal of NO<sub>x</sub> from flue gas. *NATO ASI Series*, 34(Part B):187–198, 1993. 1610.